

X-ray high-resolution diffraction and reflectivity studies of defects related to the mechanical treatment of  $\text{NdGaO}_3$  single crystals

This article has been downloaded from IOPscience. Please scroll down to see the full text article.

1998 J. Phys.: Condens. Matter 10 6065

(<http://iopscience.iop.org/0953-8984/10/27/007>)

View [the table of contents for this issue](#), or go to the [journal homepage](#) for more

Download details:

IP Address: 171.66.16.209

The article was downloaded on 14/05/2010 at 16:35

Please note that [terms and conditions apply](#).

# X-ray high-resolution diffraction and reflectivity studies of defects related to the mechanical treatment of NdGaO<sub>3</sub> single crystals

K Mazur†, J Sass† and F Eichhorn‡

† Institute of Electronic Materials Technology, ul. Wólczyńska 133, Pl-01-919 Warsaw, Poland

‡ Institut für Ionenstrahlphysik und Materialforschung des Forschungszentrum, Rossendorf, D-01-314 Dresden, Germany

Received 25 February 1998, in final form 30 April 1998

**Abstract.** Triple-crystal x-ray diffractometry and x-ray reflectometry have been used to determine defects in NdGaO<sub>3</sub> epi-ready wafers caused by mechanical treatment. Reciprocal space maps around the 400 lattice point were separately made for mechanically polished wafers before and after etching treatment. The lattice imperfections have been studied by measuring the diffuse scattering. The surface morphology has been controlled by means of x-ray reflectometry. It was shown that measurements of diffuse scattering could be made with good sensitivity in a reasonable time when there was a moderate difference between the  $d$  spacing of the sample and the monochromator.

## 1. Introduction

Neodymium gallium perovskite single crystals are a suitable substrate material for the growth of untwinned (001) oriented YBa<sub>2</sub>Cu<sub>3</sub>O<sub>*x*</sub> thin films [1, 2]. In addition NdGaO<sub>3</sub> is proposed as a substrate for the growth of GaN epitaxial layers. It has an orthorhombic structure isostructural to GdFeO<sub>3</sub> with lattice constants  $a = 5.428 \text{ \AA}$ ,  $b = 5.498 \text{ \AA}$  and  $c = 7.710 \text{ \AA}$ . Besides the structure matching, good quality epilayers can be grown only on crystallographically perfect substrates with well prepared smooth and damage free surfaces.

X-ray diffuse scattering has been used as a powerful method to study different lattice defects in crystals. It is known that the x-ray diffuse scattering from damaged crystals [3] and from those containing process-induced defects [4] can be observed using a triple-crystal diffractometer (TCD) in the parallel ( $+n, -n, +n$ ) setting.

In the present work it is shown that diffuse scattering measurements are possible with good sensitivity and reasonable speed when the reflection of the sample is not the same as that of the monochromator (i.e. for a moderate difference in the sample and monochromator interplanar spacings  $d_{hkl}$ ). For this work a TCD arrangement equipped with a conventional x-ray tube (1.5 kW) was used. The two-dimensional x-ray high-resolution diffraction measurements were applied for the structural characterization of the surfaces of NdGaO<sub>3</sub> single crystal, epi-ready wafers.

The x-ray reflectivity measurements are used to characterize surfaces on a nanometre scale. They can reveal the electron density distribution along the surface normal and the surface roughness.

## 2. Experiment

The NdGaO<sub>3</sub> twin-free specimens were grown using the Czochralski technique at ITME Warsaw. They were mechanically polished and then etched in H<sub>3</sub>PO<sub>4</sub> with H<sub>2</sub>O (1:1) to remove the surface damage. The thickness of the removed layers was above 3 μm. The two-dimensional x-ray diffraction and x-ray reflectometry measurements were performed after the mechanical polishing, as well as after the etching procedure.

### 2.1. X-ray high-resolution diffraction studies

The two-dimensional x-ray diffraction analyses of nearly perfect crystals can reveal the kinematical diffraction caused by lattice imperfections in addition to the dynamical diffraction. The dynamical and kinematical diffraction give different patterns of the equal-intensity contours in reciprocal lattice space. The dynamical diffraction produces characteristic streak patterns while the kinematical diffraction forms various patterns depending on the type of lattice imperfection.

The separate measurements of kinematical and dynamical diffraction near the reciprocal lattice point can be accomplished using high-resolution TCD (ITME Warsaw) with parallel (+*n*, −*n*, +*n*) setting [3,5]. When the reflecting planes of the sample and monochromator have a different interplanar spacing special care must be taken to minimize the dispersion effect. Usually a grooved four-reflection Ge 220 monochromator is applied with beam divergence 12 in and the wavelength dispersion  $\Delta\lambda/\lambda = 1.43 \times 10^{-4}$ . However, for the applications that require a higher intensity, this solution is not advisable. For the present measurement of very weak diffuse scattering the TCD used: (i) the line focus of the x-ray tube  $f = 0.1$  mm (instead of the point one), (ii) a primary beam flat monochromator Ge(400) followed by a 0.05 mm slit at 130 mm distance and (iii) a Ge(400) channel cut analyser in front of the counter. The vertical divergence is reduced by means of a primary beam Soller slit as shown in figure 1 [6]. This arrangement allows one to obtain a well monochromatized and collimated high-intensity primary beam with wavelength dispersion  $\Delta\lambda/\lambda \simeq 2.8 \times 10^{-4}$  (the difference in wavelength between  $K_{\alpha 1}$  and  $K_{\alpha 2}$  spectral lines for Cu  $K\alpha$  radiation  $\Delta\lambda = 3.8 \times 10^{-3}$  Å).

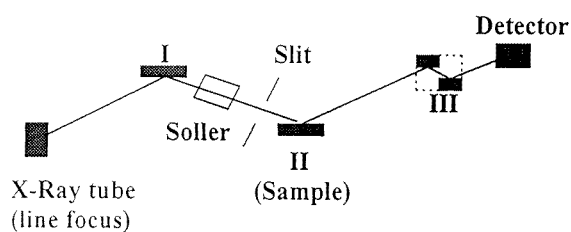


**Figure 1.** Scheme of presently used x-ray high-resolution diffractometer.

The measurements of intensity of more than  $10^4$  counts  $s^{-1}$  are easily achieved with the presented set-up at 1 kW (background  $<1$  count  $s^{-1}$ ). The higher intensity of the primary beam in the TCD presented above is obtained at the expense of a larger wavelength dispersion and increased beam divergence (37 in). The TDC resolution depends on the last two parameters. Generally, the measured scattering function is a convolution of the scattering function of the monochromator and that of the sample having regard to spectral dispersion  $\Delta\gamma$ . Assuming the Gaussian form of scattering functions with FWHM (the full

width at half maximum) equal to  $\omega_m$  and  $\omega_k$  the measured curve is characterized by the FWHM equal to

$$\omega_S = (\omega_m^2 + \omega_k^2 + \Delta\gamma^2)^{1/2} \quad (1)$$

where  $\omega_m$  is the intrinsic FWHM of the monochromator from the dynamical diffraction theory,  $\omega_k$  the intrinsic FWHM of sample from the dynamical theory and  $\Delta\gamma$  the spectral dispersion

$$\Delta\gamma = (\Delta\lambda/\lambda)(|\tan\theta_1 - \tan\theta_2|) \quad (2)$$

where  $\theta_1$  is the monochromator Bragg angle and  $\theta_2$  the sample Bragg angle.

By the dynamical theory of diffraction, one obtains the FWHM of the scattering function is given by

$$\omega_{hkl} = (2C|\chi_{hkl}|/\sin 2\theta)(\sin\beta \sin\alpha)^{1/2} \quad (3)$$

where  $C$  is the polarization factor ( $C = 1$ ),  $\alpha$  the incident angle,  $\beta$  the exit angle and  $\theta$  the Bragg angle. The crystal polarizability for Cu K $\alpha$  radiation is equal to

$$|\chi_{hkl}^{Cu}| = 2.11 \times 10^{-5} |F_{hkl}|/V [\text{\AA}] \quad (4)$$

where  $F_{hkl}$  is the structure factor and  $V$  the volume of the unit cell.

## 2.2. Reflectivity studies

The morphology of surfaces was characterized with the specular reflectivity. According to Sinha [7] the root mean square roughness  $\sigma$  is a good parameter for describing the surface morphology, provided there are no incoherent components in the entire reflected beam. The rocking curve was recorded with counter slit 0.1 mm at fixed counter position  $2\theta = 0.4^\circ$  (figure 2). We have stated, that the NdGaO<sub>3</sub>(000) rocking curve was very narrow, symmetrical and tailless.

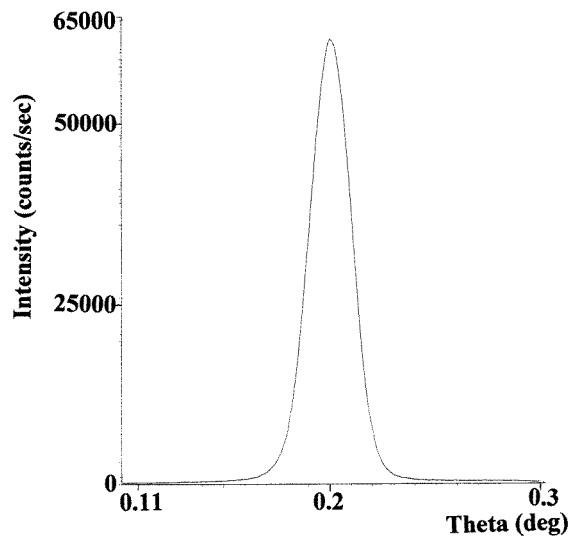


Figure 2. Rocking curve (000) of NdGaO<sub>3</sub> ( $2\theta = 0.4^\circ$ ).

Studies of specular reflectivity ( $\theta/2\theta$  scan) of the samples previously investigated with x-ray high-resolution diffraction were done with a Siemens D 5000 x-ray reflectometer at the IIM Forschungszentrum Rossendorf.

The intensity of the specular reflectivity sharply drops at the critical angle  $\theta_c$ .

$$\theta_c = (|\chi_{000}^{Cu}|)^{1/2} \quad (5)$$

where  $\chi_{000}^{Cu}$  is the complex crystal polarizability (see (4)). For the incident angle  $\theta > \theta_c$  the form of the reflectivity curve depends on the surface roughness of the sample. The penetration depth of x-rays ( $t \simeq 40$  Å for Cu  $K\alpha$ ) is much smaller than for the high-angle diffraction case.

### 3. Results and discussion

The TCD equipment enabled the measurement of Bragg reflections from sample lattice planes with a moderate difference of interplanar spacing  $d_{hkl}$  with respect to the Ge  $d_{004}$ . NdGaO<sub>3</sub> 400 reflection, symmetric Bragg case (Cu  $K\alpha$ ) were investigated. In this case close to the Bragg condition the penetration depth was only  $t = 3.5$   $\mu\text{m}$ . This small value is due to the Nd absorption edge for the Cu  $K\alpha_1$ . It allowed us to estimate quite precisely the thickness of damaged layer. The x-ray high-resolution measurements were carried out by  $\omega$  scans with different  $2\theta$  offsets ( $\omega = \text{variable}$ ,  $2\theta = \text{constant}$ ). The variation of the sample reflectivity with the angle  $\omega$  with  $2\theta$  fixed is usually called the differential rocking curve (DRC).

The end point of the diffraction vector  $H$  is on the Ewald sphere and the rotation of the specimen corresponds to the shift of the Ewald sphere as shown in figure 3. Making a series of DRC measurements on the sample in the vicinity of the reciprocal lattice point with different detector positions  $2\theta$  we obtained two-dimensional intensity distribution in the reciprocal lattice space. The diffraction intensities were measured step by step with fixed time counting (2 s).

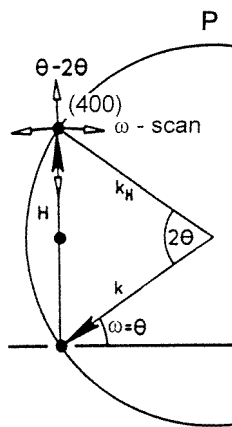


**Figure 3.** The principle of  $\omega$ -scan in reciprocal space.  $H$ , diffraction vector;  $P$ , Ewald sphere;  $k$ , incident wavevector;  $k_H$ , diffracted wavevector;  $\theta$ , Bragg angle.

The reciprocal space map in ( $\omega/2\theta$ ,  $\Delta\omega$ ) co-ordinates from the mechanically polished sample is presented in figure 4. The intensity distribution around the 400 reciprocal lattice point of NdGaO<sub>3</sub> is presented as equal-intensity contours. The

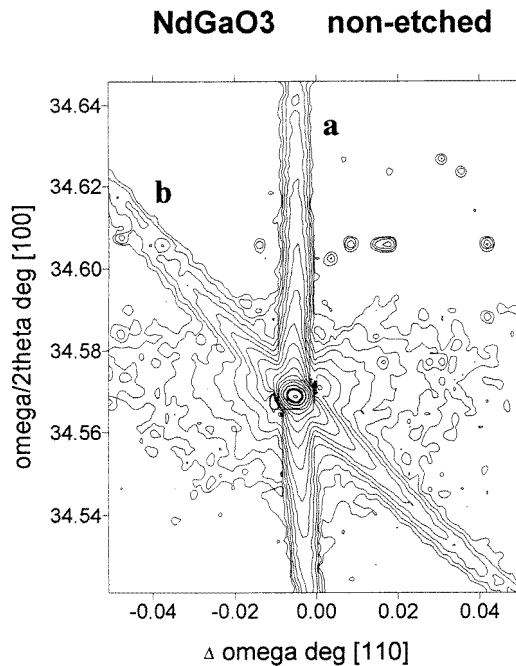


**Figure 4.** Reciprocal space mapping of NdGaO<sub>3</sub>(400) Cu K $\alpha$ ; surface state after mechanical polishing, (a) main streak; (b) pseudo-streak; the last iso-intensity contour corresponds to 1 count s<sup>-1</sup>.

intensity ratio of neighbouring contours is 1:2. The last contour in figure 4 represents the intensity 1 count s<sup>-1</sup>. The contour corresponding to the intensity of the half-maximum value is marked by the thick line. It is round in shape with the diameter equal to 13.5 arc sec. The calculated intrinsic FWHM for NdGaO<sub>3</sub>  $\omega_{400} = 9.5$  arc sec, and according to equations (1)–(4)  $\omega_s = 12.5$  arc sec.

These contours formed the dynamical streak, the dynamical pseudo-streak (due to primary beam monochromator) and quasi-circular patterns. The circular intensity contours in the reciprocal space maps are caused by residual surface damage after lapping and thermal diffuse scattering [3, 5]. We observed that these quasi-circular patterns are not azimuthally dependent. After etching the NdGaO<sub>3</sub> sample the peak intensity was 20% higher than the peak intensity of the sample before etching and the circular intensity contours vanished (figure 5). The quasi-circular contours are due to the kinematical diffraction (diffuse scattering). The kinematical diffraction can be affected by a slight lattice distortion (mosaic-like structure) of the samples. This means that the etching solution removes the damage (caused by mechanical treatment) of the crystalline surface layer. Moreover, this shows that the diffuse scattering is caused by the surface damage with no contribution of volume defects.

The specular reflectivity measurements ( $\theta/2\theta$  scan) for both surface states of NdGaO<sub>3</sub> before and after etching are presented in figure 6. The resulting values for roughness ( $\sigma$ ) and density from the fitting process with the Refsim program (commercial Siemens software) are given in the inset in figure 6. It should be noticed that the value  $\theta_c^{exp}$  agrees well with value derived from (5) and no oxide layer on top of the wafer surface was observed for the both cases. The reflectivity value of roughness ( $\sigma$ ) from the as-polished sample was

### NdGaO<sub>3</sub> etched

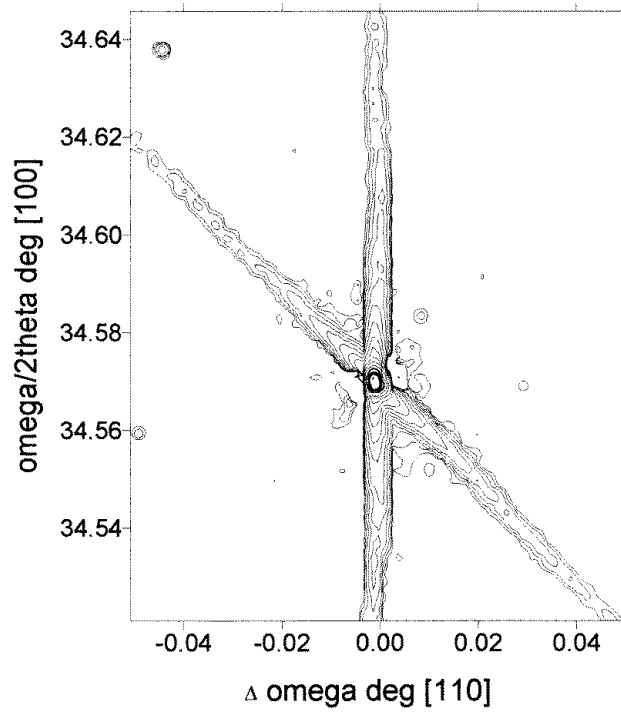


Figure 5. Reciprocal space mapping of NdGaO<sub>3</sub>(400) Cu K $\alpha$ ; surface state after etching.

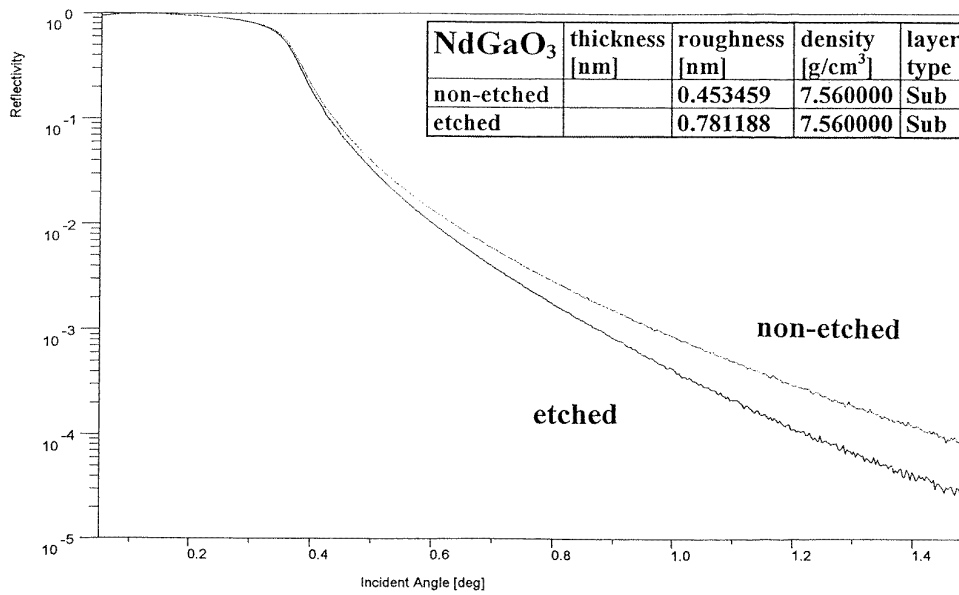


Figure 6. Reflectivity curves of NdGaO<sub>3</sub> wafer before and after etching.

equal to  $0.45 \pm 0.05$  nm. After the etching procedure the roughness of the sample increased to  $0.78 \pm 0.05$  nm. This means that the etching solution removes the damage (caused by mechanical treatment) of the crystalline surface layer, but produces a rougher surface.

Summarizing: (i) TCD and reflectivity measurements are appropriate tools for studying defects related to mechanical treatment; (ii) the etching procedure compromises between residual surface damage and surface morphology; (iii) no oxide layer on the top of the wafer surface was observed.

### Acknowledgments

The authors are indebted to Professor A Turos for critical comments to improve the manuscript. The Polish Committee of Scientific Researches KBN (grant 792/TO8/96/11) supported this work.

### References

- [1] Young K H and Sun J Z 1991 *Appl. Phys. Lett.* **59** 2448
- [2] Mazur K, Sass J, Giersz W, Reiche P and Schell N 1997 *Acta Phys. Pol. A* **92**
- [3] Iida A and Kohra K 1979 *Phys. Status Solidi a* **51** 533–42
- [4] Servidori M and Fabbri R 1993 *J. Phys. D: Appl. Phys.* **26** A22–A28
- [5] Zaumseil P and Winter U 1982 *Phys. Status Solidi a* **70** 497–505
- [6] Sass J 1994 *Mater. Elektron. T* **22** 19–34
- [7] Sinha S K 1996 *Acta Phys. Pol. A* **89** 21